



# The synthesis and spectroscopic investigation of dichromophoric hemicyanine dyes

Beata Jędrzejewska\*, Artur Rudnicki<sup>1</sup>

University of Technology and Life Sciences, Faculty of Chemical Technology and Engineering, Seminaryjna 3, 85-326 Bydgoszcz, Poland

## ARTICLE INFO

### Article history:

Received 12 March 2008  
Received in revised form 17 July 2008  
Accepted 19 July 2008  
Available online 20 August 2008

### Keywords:

Dichromophoric hemicyanine dye  
Synthesis  
Absorption and emission spectra  
The Stokes shift

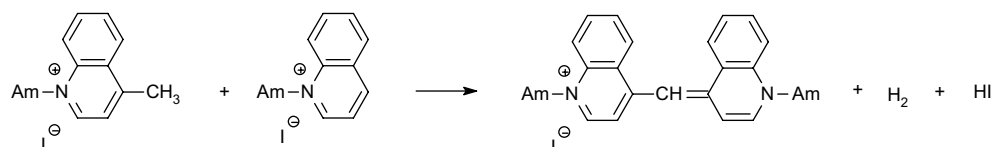
## ABSTRACT

Alkane  $\alpha,\gamma$ -bis[4-methylpyridinium] diiodide and alkane  $\alpha,\gamma$ -bis[4-methylquinolinium] diiodide were prepared and used as starting materials in the synthesis of dichromophoric cyanine dyes. Structural confirmation of the synthesized dyes was carried out by <sup>1</sup>H NMR, MS spectroscopy and elemental analysis. The electronic absorption and the emission spectra for all the hemicyanines were measured in four organic solvents of varying polarity. All derivatives absorb in the region of about 500 nm and have molar absorptivity of about  $10^4 \text{ M}^{-1} \text{ cm}^{-1}$ . The absorption spectra of tested compounds are affected by their structure i.e. the structure of dialkyl(aryl)amino group, the electron acceptor part of the dye and the linker between two identical hemicyanine chromophores. The fluorescence bands' positions, in contrast to the absorption, are strongly affected by the solvent polarity.

© 2008 Elsevier Ltd. All rights reserved.

## 1. Introduction

The first cyanine dyes were obtained in 1856 by Greville Williams [1]. The dye named as Cyanine or Quinoline Blue was made by heating the isoamyl iodides of quinoline and lepidine with caustic alkali:



While the name Cyanine denoted the deep blue color of Williams' dye, the cyanine dyes now cover nearly the whole of the color range; but they belong to a relatively compact group, considering that many thousands have been already synthesized. Extensive synthetic procedures for generating cyanine dyes of diverse molecular structure were developed so far [2–4]. A general method for the synthesis of stilbazolium dyes (hemicyanines) involves a condensation of a 2- or 4-methyl quaternary salt of the

nitrogen heterocycle with substituted benzaldehyde in the presence of suitable base [5–7]. Synthesis of dyes, which would be stable against light, heat, oxygen and ozone is important from practical viewpoints.

Polymethine cyanine dyes have found various applications as photographic sensitizers for both color and black and white films

and textile dyes. They are also useful as photosensitizers in blue green light and as analytical reagents. Hemicyanine dyes which possess the electron pushing (donor) group on one end of a molecule and the electron withdrawing (acceptor) group on the other end have found an successful application in science and technology. These chromophores are common fluorescence probes used in biochemistry and biophysical area [8]. They are also very commonly applied to lasers [9], electronics [10], and nonlinear optics [11].

In this paper, we present an extension of our former work [12–16]. We describe the synthesis of a series of dichromophoric stilbene-type derivatives in which a terminal substituted amino groups are used as electron donors. The effect of the dyes' structure

\* Corresponding author. Tel.: +48 52 374 9034; fax: +48 52 374 9009.  
E-mail address: [beata@utp.edu.pl](mailto:beata@utp.edu.pl) (B. Jędrzejewska).

<sup>1</sup> Master degree student of University of Technology and Life Sciences.

on their spectroscopic properties is discussed as well. The results obtained for dichromophoric dyes are compared to structurally related monochromophoric hemicyanines. It is necessary to emphasize that some of the hemicyanine dyes are known in literature [17–21], e.g. monochromophoric compounds (**P7**, **P8**, **D7**) and bischromophoric dyes: **P1–P3** were previously synthesized and used for different purposes by others.

## 2. Experimental

### 2.1. Measurements

All starting reagents and solvents (reagent grade) were purchased from either Aldrich Chemical Co. or Lancaster and were used without further purification. Aldehydes as substrates for the synthesis of dichromophoric dyes were synthesized according to the procedure given by Gawinecki et al. [17].

The  $^1\text{H}$  NMR spectra were recorded with the use of a Varian Gemini 200 spectrometer operating at 200 MHz. Dimethylsulfoxide ( $\text{DMSO}-d_6$ ) was used as the solvent and tetramethylsilane (TMS) as the internal standard.

The elemental analysis was made with a Vario Macro 11.45-0000 (Elementar Analysensysteme GmbH, Germany) operating with the software VARIOEL (version 5.14.4.22).

Lo-Res Mass Data were obtained on a Spectrometer AMD Intetra Mass AMD 604 using method known as Liquid Secondary Ion Mass Spectrometry (LSIMS) involving the bombardment of a solid spot of the analyte/matrix mixture by a fast particle beam (primary ions,  $\text{Cs}^+$  at 35 keV).

Melting points (uncorrected) were determined on the Boëthius apparatus.

For the measurements of the electronic absorption and emission spectra the  $1.0 \times 10^{-5}$  M dye solutions in *N,N*-dimethylformamide (DMF), 1-methyl-2-pyrrolidinone (MP), ethyl acetate (EtOAc) and tetrahydrofuran (THF) were prepared. Absorption spectra were recorded at room temperature using a Shimadzu UV–vis Multispec-1501 spectrophotometer, and fluorescence spectra were obtained with a Hitachi F-4500 spectrofluorimeter. The fluorescence measurements were performed at an ambient temperature.

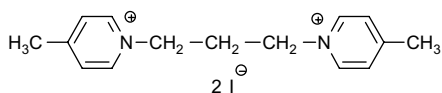
### 2.2. Synthetic procedure

All dyes discussed in this paper were obtained by the known methods described in literature [6,7,12,17–21].

#### 2.2.1. Alkane $\alpha,\gamma$ -bis[4-methylpyridinium] diiodide and alkane $\alpha,\gamma$ -bis[4-methylquinolinium] diiodide

To a solution of  $\alpha,\gamma$ -diiodoalkane (0.1 mol) in anhydrous ethanol (50 mL) either  $\gamma$ -picoline (0.2 mol) or 4-methylquinoline (0.2 mol) was added. The reaction mixture was refluxed for 6 h and then the solution was concentrated in vacuum to give a white or yellow solid [12,19].

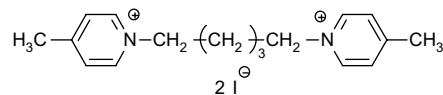
##### 2.2.1.1. Propane 1,3-bis[4-methylpyridinium] diiodide.



$^1\text{H}$  NMR ( $\text{DMSO}-d_6$ )  $\delta$  (ppm): 2.076 (m, 2H,  $-\text{CH}_2-$ ), 2.618 (s, 6H,  $-\text{CH}_3$ ), 4.621 (t, 4H,  $\text{N}^+\text{CH}_2-$ ), 8.010–8.041 (d,  $J = 6.2$  Hz, 4H, Pyr), 8.890–8.925 (d,  $J = 7.0$  Hz, 4H, Pyr).

$^{13}\text{C}$  NMR ( $\text{DMSO}-d_6$ )  $\delta$  (ppm): 21.605 ( $-\text{CH}_3$ ), 31.513, 56.639 ( $-\text{CH}_2-$ ), 128.544, 143.853 (ArH), 159.216 (Ar).

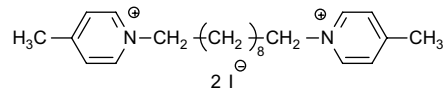
##### 2.2.1.2. Pentane 1,5-bis[4-methylpyridinium] diiodide.



$^1\text{H}$  NMR ( $\text{DMSO}-d_6$ )  $\delta$  (ppm): 1.279 (m, 2H,  $-\text{CH}_2-$ ), 1.929 (m, 4H,  $-\text{CH}_2-$ ), 2.607 (s, 6H,  $-\text{CH}_3$ ), 4.519 (t, 4H,  $\text{N}^+\text{CH}_2-$ ), 7.980–8.011 (d,  $J = 6.2$  Hz, 4H, Pyr), 8.898–8.933 (d,  $J = 7.0$  Hz, 4H, Pyr).

$^{13}\text{C}$  NMR ( $\text{DMSO}-d_6$ )  $\delta$  (ppm): 21.511 ( $-\text{CH}_3$ ), 21.746, 29.814, 59.424 ( $-\text{CH}_2-$ ), 128.430, 143.732 (ArH), 158.874 (Ar).

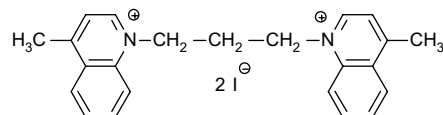
##### 2.2.1.3. Decane 1,10-bis[4-methylpyridinium] diiodide.



$^1\text{H}$  NMR ( $\text{DMSO}-d_6$ )  $\delta$  (ppm): 1.234 (m, 12H,  $-\text{CH}_2-$ ), 1.897 (m, 4H,  $-\text{CH}_2-$ ), 2.597 (s, 6H,  $-\text{CH}_3$ ), 4.505 (t, 4H,  $\text{N}^+\text{CH}_2-$ ), 7.963–7.992 (d,  $J = 5.8$  Hz, 4H, Pyr), 8.901–8.934 (d,  $J = 6.6$  Hz, 4H, Pyr).

$^{13}\text{C}$  NMR ( $\text{DMSO}-d_6$ )  $\delta$  (ppm): 21.533 ( $-\text{CH}_3$ ), 25.334, 28.338, 28.664, 30.613, 59.856 ( $-\text{CH}_2-$ ), 128.392, 143.679 (ArH), 158.768 (Ar).

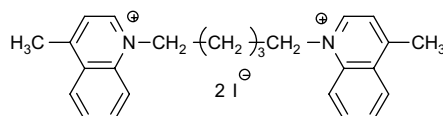
##### 2.2.1.4. Propane 1,3-bis[4-methylquinolinium] diiodide.



$^1\text{H}$  NMR ( $\text{DMSO}-d_6$ )  $\delta$  (ppm): 2.688 (m, 2H,  $-\text{CH}_2-$ ), 3.000 (s, 6H,  $-\text{CH}_3$ ), 5.025 (t, 4H,  $\text{N}^+\text{CH}_2-$ ), 8.011–8.055 (d,  $J = 8.8$  Hz, 2H, Ar), 8.088–8.120 (d,  $J = 6.4$  Hz, 2H, Ar), 8.271 (m, 2H, Ar), 8.527 (t, 2H, Ar), 8.714–8.758 (d,  $J = 8.8$  Hz, 2H, Ar), 9.359–9.388 (d,  $J = 5.4$  Hz, 2H, Ar), 9.406–9.439 (d,  $J = 6.6$  Hz, 2H, Ar).

$^{13}\text{C}$  NMR ( $\text{DMSO}-d_6$ )  $\delta$  (ppm): 33.154, 57.488 ( $-\text{CH}_2-$ ), 19.917 ( $-\text{CH}_3$ ), 119.129, 122.744, 127.195, 129.553, 135.143, 148.598 (ArH), 158.758 (Ar).

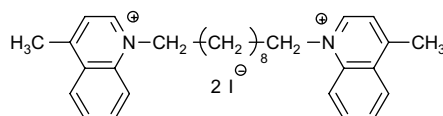
##### 2.2.1.5. Pentane 1,5-bis[4-methylquinolinium] diiodide.



$^1\text{H}$  NMR ( $\text{DMSO}-d_6$ )  $\delta$  (ppm): 1.498 (m, 2H,  $-\text{CH}_2-$ ), 2.007 (m, 4H,  $-\text{CH}_2-$ ), 3.007 (s, 6H,  $-\text{CH}_3$ ), 4.996 (t, 4H,  $\text{N}^+\text{CH}_2-$ ), 8.055–8.088 (d,  $J = 6.6$  Hz, 4H, Ar), 8.241 (t, 2H, Ar), 8.546 (m, 4H, Ar), 9.384–9.417 (d,  $J = 6.6$  Hz, 2H, Ar).

$^{13}\text{C}$  NMR ( $\text{DMSO}-d_6$ )  $\delta$  (ppm): 22.776, 28.875, 56.614 ( $-\text{CH}_2-$ ), 19.953 ( $-\text{CH}_3$ ), 119.430, 122.634, 127.141, 129.571, 135.106, 148.252 (ArH), 158.457 (Ar).

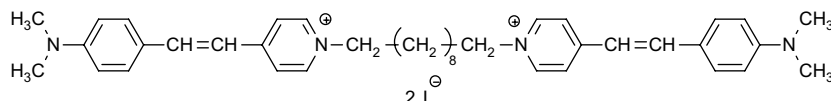
##### 2.2.1.6. Decane 1,10-bis[4-methylquinolinium] diiodide.



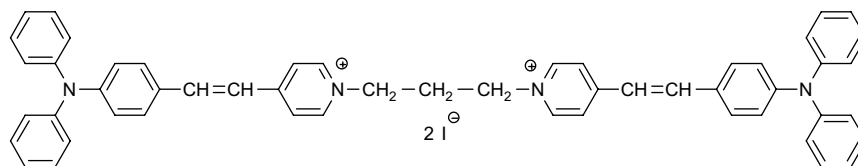
$^1\text{H}$  NMR ( $\text{DMSO}-d_6$ )  $\delta$  (ppm): 1.230 (m, 12H,  $-\text{CH}_2-$ ), 1.915 (m, 4H,  $-\text{CH}_2-$ ), 2.996 (s, 6H,  $-\text{CH}_3$ ), 4.978 (t, 4H,  $\text{N}^+\text{CH}_2-$ ), 8.044–8.077 (d,  $J = 6.6$  Hz, 4H, Ar), 8.249 (t, 2H, Ar), 8.553 (t, 4H, Ar), 9.362–9.395 (d,  $J = 6.6$  Hz, 2H, Ar).

$^{13}\text{C}$  NMR (DMSO- $d_6$ )  $\delta$  (ppm): 25.807, 28.493, 28.784, 29.503, 56.960 ( $-\text{CH}_2-$ ), 19.844 ( $-\text{CH}_3$ ), 119.348, 122.616, 127.141, 129.544, 135.070, 148.234 (ArH), 158.457 (Ar).

## 2.2.2. General procedure for the synthesis of 1,3-bis[4-(4-(dialkylaminophenyl)ethenyl)pyridinyl]-alkane diiodide derivatives

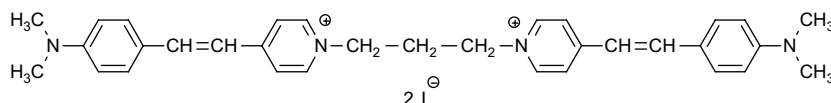


$\alpha,\gamma$ -Bis[4-(4-(dialkylaminophenyl)ethenyl)pyridinyl]-alkane diiodide or  $\alpha,\gamma$ -bis[4-(4-(dialkylaminophenyl)ethenyl)quinolinyl]-alkane diiodide derivatives were obtained by refluxing (1–2 h) a proper *p*-aminobenzaldehyde (4 mmol) with either alkane  $\alpha,\gamma$ -bis[4-methylpyridinium iodide] or alkane  $\alpha,\gamma$ -bis[4-methylquinolinium iodide] (2 mmol) in alcohol (20 mL) in the presence of piperidine (few drops). The precipitate formed after cooling down the reaction mixture was filtered and then crystallized from MeOH/isopropyl alcohol to afford the desired dye [7,12,15]. The products



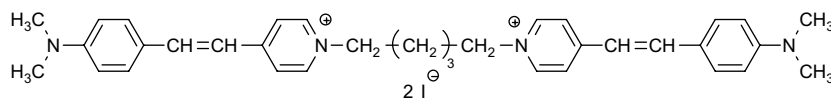
were identified by  $^1\text{H}$  NMR, MS spectroscopy and elemental analysis.

### 2.2.2.1. Dye **P1** –1,3-bis[4-(2-(4-(N,N-dimethylamino)phenyl)ethenyl)pyridinyl]-propane diiodide.

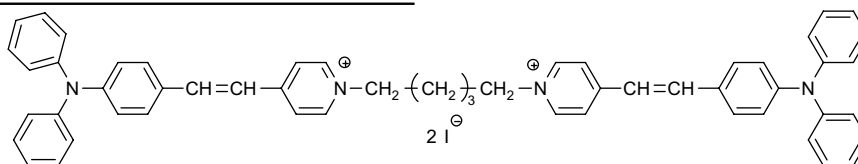


$^1\text{H}$  NMR (DMSO- $d_6$ )  $\delta$  (ppm): 2.618 (m, 2H,  $-\text{CH}_2-$ ), 3.020 (s, 12H, N- $\text{CH}_3$ ), 4.530 (t, 4H, N $^+\text{CH}_2-$ ), 7.142–7.222 (d,  $J = 16.0$  Hz, 2H,  $-\text{CH}=\text{}$ ), 7.903–7.983 (d,  $J = 16.0$  Hz, 2H,  $-\text{CH}=\text{}$ ), 6.750–6.795 (d,  $J = 9.0$  Hz, 4H, Ar), 7.565–7.609 (d,  $J = 8.8$  Hz, 4H, Ar), 8.063–8.097 (d,  $J = 6.8$  Hz, 4H, Pyr), 8.729–8.763 (d,  $J = 6.8$  Hz, 4H, Pyr).

### 2.2.2.2. Dye **P2** –1,5-bis[4-(2-(4-(N,N-dimethylamino)phenyl)ethenyl)pyridinyl]-pentane diiodide.



$^1\text{H}$  NMR (DMSO- $d_6$ )  $\delta$  (ppm): 1.219 (m, 2H,  $-\text{CH}_2-$ ), 1.938 (m, 4H,  $-\text{CH}_2-$ ), 3.018 (s, 12H, N- $\text{CH}_3$ ), 4.421 (t, 4H, N $^+\text{CH}_2-$ ), 7.116–7.197



(d,  $J = 16.2$  Hz, 2H,  $-\text{CH}=\text{}$ ), 7.884–7.965 (d,  $J = 16.2$  Hz, 2H,  $-\text{CH}=\text{}$ ), 6.740–6.783 (d,  $J = 8.6$  Hz, 4H, Ar), 7.547–7.591 (d,  $J = 8.8$  Hz, 4H, Ar), 8.046–8.077 (d,  $J = 6.2$  Hz, 4H, Pyr), 8.730–8.762 (d,  $J = 6.2$  Hz, 4H, Pyr).

### 2.2.2.3. Dye **P3** –1,10-bis[4-(2-(4-(N,N-dimethylamino)phenyl)ethenyl)pyridinyl]-decane diiodide.

$^1\text{H}$  NMR (DMSO- $d_6$ )  $\delta$  (ppm): 1.252 (m, 12H,  $-\text{CH}_2-$ ), 1.856 (m, 4H,  $-\text{CH}_2-$ ), 3.015 (s, 12H, N- $\text{CH}_3$ ), 4.389 (t, 4H, N $^+\text{CH}_2-$ ), 7.121–7.202 (d,  $J = 16.2$  Hz, 2H,  $-\text{CH}=\text{}$ ), 7.872–7.953 (d,  $J = 16.2$  Hz, 2H,  $-\text{CH}=\text{}$ ), 6.757–6.801 (d,  $J = 8.8$  Hz, 4H, Ar), 7.563–7.608 (d,  $J = 9.0$  Hz, 4H, Ar), 8.030–8.063 (d,  $J = 6.6$  Hz, 4H, Pyr), 8.731–8.764 (d,  $J = 6.6$  Hz, 4H, Pyr).

### 2.2.2.4. Dye **P4** –1,3-bis[4-(2-(4-(N,N-diphenylamino)phenyl)ethenyl)pyridinyl]-propane diiodide.

$^1\text{H}$  NMR (DMSO- $d_6$ )  $\delta$  (ppm): 2.890 (m, 2H,  $-\text{CH}_2-$ ), 4.567 (t, 4H, N $^+\text{CH}_2-$ ), 7.201–7.271 (d,  $J = 14.0$  Hz, 2H,  $-\text{CH}=\text{}$ ), 7.934–8.007 (d,

$J = 14.6$  Hz, 2H,  $-\text{CH}=\text{}$ ), 6.923 (m, 6H, Ar), 7.128 (t, 10H, Ar), 7.340–7.381 (d,  $J = 8.0$  Hz, 8H, Ar), 7.593–7.637 (d,  $J = 8.8$  Hz, 4H, Ar), 8.064–8.097 (d,  $J = 6.6$  Hz, 2H, Pyr), 8.161–8.194 (d,  $J = 6.6$  Hz, 2H, Pyr), 8.816–8.849 (d,  $J = 6.6$  Hz, 2H, Pyr), 9.925–9.959 (d,  $J = 6.8$  Hz, 2H, Pyr).

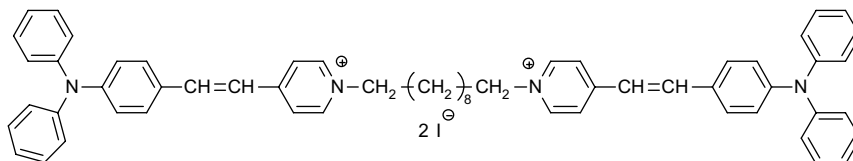
Low resolution MS,  $m/z$ : calc. 738.97  $[\text{M} - 2\text{I}]^{2+}$ , measured 739.4  $[\text{M} - 2\text{I}]^{2+}$ .

### 2.2.2.5. Dye **P5** –1,5-bis[4-(2-(4-(N,N-diphenylamino)phenyl)ethenyl)pyridinyl]-pentane diiodide.

$^1\text{H}$  NMR (DMSO- $d_6$ )  $\delta$  (ppm): 1.269 (m, 2H,  $-\text{CH}_2-$ ), 1.912 (m, 4H,  $-\text{CH}_2-$ ), 4.469 (t, 4H,  $\text{N}^+\text{CH}_2-$ ), 7.190–7.267 (d,  $J = 15.4$  Hz, 2H,  $-\text{CH}=\text{}$ ), 7.919–8.003 (d,  $J = 16.8$  Hz, 2H,  $-\text{CH}=\text{}$ ), 6.908–6.952 (d,  $J = 8.8$  Hz, 8H, Ar), 7.121 (t, 10H, Ar), 7.333–7.373 (d,  $J = 8.0$  Hz, 6H, Ar), 7.589–7.630 (d,  $J = 8.2$  Hz, 4H, Ar), 8.029–8.062 (d,  $J = 6.6$  Hz, 2H, Pyr), 8.150–8.183 (d,  $J = 6.6$  Hz, 2H, Pyr), 8.838–8.871 (d,  $J = 6.6$  Hz, 2H, Pyr), 8.945–8.963 (2H, Pyr).

Low resolution MS,  $m/z$ : calc. 767.02  $[\text{M} - 2\text{I}]^{2+}$ , measured 767.9  $[\text{M} - 2\text{I}]^{2+}$ .

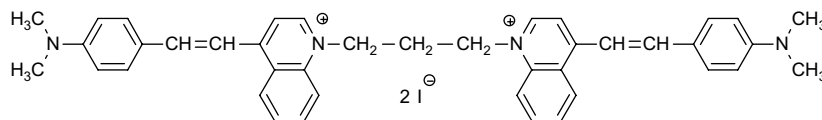
2.2.2.6. Dye **P6** – 1,10-bis[4-(2-(4-(N,N-dimethylamino)phenyl)ethenyl)pyridinyl]-decane diiodide.



$^1\text{H}$  NMR (DMSO- $d_6$ )  $\delta$  (ppm): 1.250 (m, 12H,  $-\text{CH}_2-$ ), 1.858 (m, 4H,  $-\text{CH}_2-$ ), 4.433 (t, 4H,  $\text{N}^+\text{CH}_2-$ ), 7.185–7.253 (d,  $J = 13.6$  Hz, 2H,  $-\text{CH}=\text{}$ ), 7.903–7.984 (d,  $J = 16.2$  Hz, 2H,  $-\text{CH}=\text{}$ ), 6.909–6.953 (d,  $J = 8.8$  Hz, 4H, Ar), 6.997–7.033 (d,  $J = 7.2$  Hz, 4H, Ar), 7.121 (t, 10H, Ar), 7.336–7.376 (d,  $J = 8.0$  Hz, 8H, Ar), 7.592–7.636 (d,  $J = 8.8$  Hz, 4H, Ar).

$^1\text{H}$  NMR (DMSO- $d_6$ )  $\delta$  (ppm): 4.205 (t, 3H,  $\text{N}^+\text{CH}_3$ ), 7.190–7.267 (d,  $J = 15.4$  Hz, 1H,  $-\text{CH}=\text{}$ ), 7.886–7.967 (d,  $J = 16.2$  Hz, 1H,  $-\text{CH}=\text{}$ ), 6.769–6.813 (d,  $J = 8.8$  Hz, 2H, Ar), 6.875–6.915 (d,  $J = 8.0$  Hz, 2H, Ar), 7.124 (t, 6H, Ar), 7.337–7.377 (d,  $J = 8.0$  Hz, 4H, Ar), 7.593–7.637 (d,  $J = 8.8$  Hz, 1H, Pyr), 7.831–7.864 (d,  $J = 6.6$  Hz, 1H, Pyr), 8.106–8.139 (d,  $J = 6.6$  Hz, 1H, Pyr), 8.740–8.776 (d,  $J = 7.2$  Hz, 1H, Pyr).

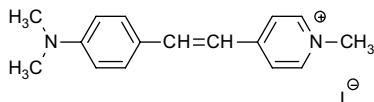
2.2.2.9. Dye **D1** – 1,3-bis[4-(2-(4-(N,N-dimethylamino)phenyl)ethenyl)quinolinyl]-propane diiodide.



4H, Ar), 8.127–8.160 (d,  $J = 6.6$  Hz, 2H, Pyr), 8.826–8.859 (d,  $J = 6.6$  Hz, 4H, Pyr).

Low resolution MS,  $m/z$ : calc. 837.16  $[\text{M} - 2\text{I}]^{2+}$ , measured 837.8  $[\text{M} - 2\text{I}]^{2+}$ .

2.2.2.7. Dye **P7** – 1-methyl-4-(4-(N,N-dimethylamino)styryl)pyridinium iodide.



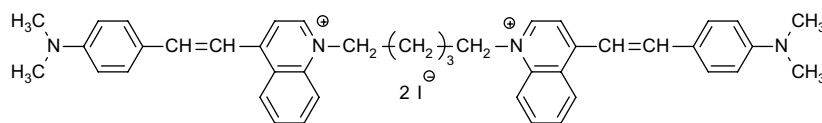
$^1\text{H}$  NMR (DMSO- $d_6$ )  $\delta$  (ppm): 3.018 (s, 6H,  $\text{N}-\text{CH}_3$ ), 4.162 (t, 3H,  $\text{N}^+\text{CH}_3$ ), 7.114–7.195 (d,  $J = 16.2$  Hz, 1H,  $-\text{CH}=\text{}$ ), 7.854–7.933 (d,  $J = 15.8$  Hz, 1H,  $-\text{CH}=\text{}$ ), 6.761–6.795 (d,  $J = 6.8$  Hz, 2H, Ar),

$^1\text{H}$  NMR (DMSO- $d_6$ )  $\delta$  (ppm): 2.671 (m, 2H,  $-\text{CH}_2-$ ), 3.073 (s, 12H,  $\text{N}-\text{CH}_3$ ), 4.905 (t, 4H,  $\text{N}^+\text{CH}_2-$ ), 7.983–8.066 (d,  $J = 16.6$  Hz, 4H,  $-\text{CH}=\text{}$ ), 6.789–6.852 (4H, Ar), 7.648–7.693 (d,  $J = 9.0$  Hz, 1H, Ar), 7.836–7.907 (2H, Ar), 8.194 (4H, Ar), 8.361 (t, 2H, Ar), 8.417–8.460 (d,  $J = 8.6$  Hz, 1H, Ar), 8.504–8.547 (d,  $J = 8.6$  Hz, 1H, Ar), 8.670–8.714 (d,  $J = 8.8$  Hz, 1H, Ar), 8.999–9.040 (d,  $J = 8.2$  Hz, 2H, Ar), 9.068–9.101 (d,  $J = 6.6$  Hz, 2H, Ar).

Low resolution MS,  $m/z$ : calc. 590.34  $[\text{M} - 2\text{I}]^{2+}$ , measured 590.5  $[\text{M} - 2\text{I}]^{2+}$ .

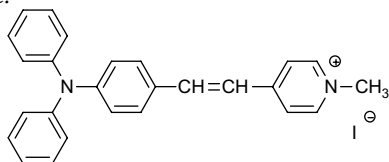
Elemental analysis: calc. 58.30% C, 5.012% H, 6.633% N, measured 52.85% C, 5.001% H, 5.926% N.

2.2.2.10. Dye **D2** – 1,5-bis[4-(2-(4-(N,N-dimethylamino)phenyl)ethenyl)quinolinyl]-pentane diiodide.



7.568–7.605 (d,  $J = 7.4$  Hz, 2H, Ar), 8.019–8.044 (d,  $J = 5.0$  Hz, 2H, Pyr), 8.654–8.682 (d,  $J = 5.6$  Hz, 2H, Pyr).

2.2.2.8. Dye **P8** – 1-methyl-4-(4-(N,N-diphenylamino)styryl)pyridinium iodide.

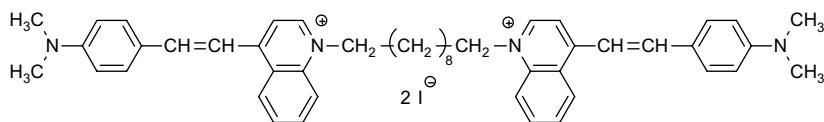


$^1\text{H}$  NMR (DMSO- $d_6$ )  $\delta$  (ppm): 1.481 (m, 2H,  $-\text{CH}_2-$ ), 1.982 (m, 4H,  $-\text{CH}_2-$ ), 3.070 (s, 12H,  $\text{N}-\text{CH}_3$ ), 4.858 (t, 4H,  $\text{N}^+\text{CH}_2-$ ), 7.901–7.980 (d,  $J = 15.8$  Hz, 4H,  $-\text{CH}=\text{}$ ), 6.759–6.841 (d,  $J = 9.2$  Hz, 4H, Ar), 7.843–7.889 (d,  $J = 9.2$  Hz, 4H, Ar), 8.156 (t, 4H, Ar), 8.304–8.337 (d,  $J = 6.6$  Hz, 2H, Ar), 8.379–8.423 (d,  $J = 8.8$  Hz, 2H, Ar), 9.000–9.042 (d,  $J = 8.4$  Hz, 2H, Ar), 9.077–9.112 (d,  $J = 7.0$  Hz, 2H, Ar).

Low resolution MS,  $m/z$ : calc. 618.37  $[\text{M} - 2\text{I}]^{2+}$ , measured 618.4  $[\text{M} - 2\text{I}]^{2+}$ .

Elemental analysis: calc. 59.183% C, 5.313% H, 6.420% N, measured 57.79% C, 5.586% H, 6.301% N.

2.2.2.11. Dye **D3** – 1,10-bis[4-(2-(4-(N,N-dimethylamino)phenyl)ethenyl)quinolinyl]-decane diiodide.



$^1\text{H}$  NMR (DMSO- $d_6$ )  $\delta$  (ppm): 1.233 (m, 12H,  $-\text{CH}_2-$ ), 1.893 (m, 4H,  $-\text{CH}_2-$ ), 3.059 (s, 12H,  $\text{N}-\text{CH}_3$ ), 4.838 (t, 4H,  $\text{N}^+\text{CH}_2-$ ), 7.949–8.031 (d,  $J = 16.4$  Hz, 4H,  $-\text{CH}=\text{CH}-$ ), 6.788–6.832 (d,  $J = 8.8$  Hz, 4H, Ar), 7.837–7.881 (d,  $J = 8.8$  Hz, 4H, Ar), 8.165 (t, 4H, Ar), 8.314–8.346 (d,  $J = 6.4$  Hz, 2H, Ar), 8.383–8.427 (d,  $J = 8.8$  Hz, 2H, Ar), 9.000–9.044 (d,  $J = 8.8$  Hz, 2H, Ar), 9.101–9.136 (d,  $J = 6.8$  Hz, 2H, Ar).

Low resolution MS,  $m/z$ : calc. 688.45  $[\text{M} - 2\text{I}]^{2+}$ , measured 688.6  $[\text{M} - 2\text{I}]^{2+}$ .

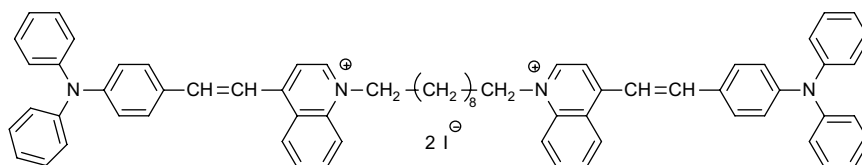
Elemental analysis: calc. 61.151% C, 5.987% H, 5.943% N, measured 60.66% C, 5.967% H, 5.878% N.

2H, Ar), 7.857–8.901 (d,  $J = 8.8$  Hz, 4H, Ar), 8.395 (t, 2H, Ar), 8.989–9.025 (d,  $J = 7.2$  Hz, 1H, Ar), 9.242–9.278 (d,  $J = 7.2$  Hz, 1H, Ar).

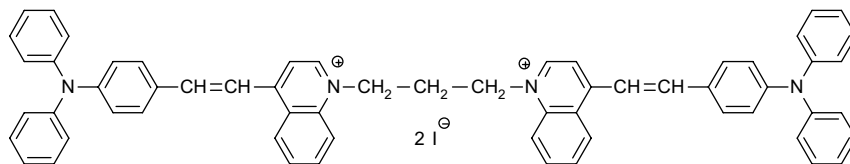
Low resolution MS,  $m/z$ : calc. 867.14  $[\text{M} - 2\text{I}]^{2+}$ , measured 867.6  $[\text{M} - 2\text{I}]^{2+}$ .

Elemental analysis: calc. 67.505% C, 4.856% H, 4.998% N, measured 62.14% C, 4.604% H, 4.884% N.

2.2.2.14. Dye **D6** – 1,10-bis[4-(2-(4-(N,N-diphenylamino)phenyl)ethenyl)quinolinyl]-decane diiodide.



2.2.2.12. Dye **D4** – 1,3-bis[4-(2-(4-(N,N-diphenylamino)phenyl)ethenyl)quinolinyl]-propane diiodide.



$^1\text{H}$  NMR (DMSO- $d_6$ )  $\delta$  (ppm): 2.685 (m, 2H,  $-\text{CH}_2-$ ), 4.985 (t, 4H,  $\text{N}^+\text{CH}_2-$ ), 8.161 (4H,  $-\text{CH}=\text{CH}-$ ), 6.853–6.890 (d,  $J = 7.4$  Hz, 2H, Ar), 6.937–6.981 (d,  $J = 8.8$  Hz, 4H, Ar), 7.164 (t, 12H, Ar), 7.399 (t, 6H, Ar), 7.692–7.729 (d,  $J = 7.4$  Hz, 2H, Ar), 7.868–7.904 (d,  $J = 7.2$  Hz, 3H, Ar), 7.963–8.036 (t, 3H, Ar), 8.234–8.267 (d,  $J = 6.6$  Hz, 2H, Ar), 8.479 (t, 2H, Ar), 8.600 (t, 2H, Ar), 9.000–9.040 (d,  $J = 8.0$  Hz, 1H, Ar), 9.271–9.300 (1H, Ar).

Elemental analysis: calc. 67.039% C, 4.614% H, 5.126% N, measured 61.09% C, 4.997% H, 5.265% N.

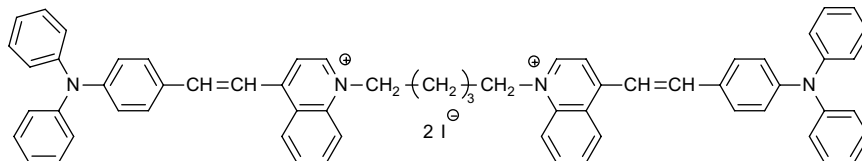
$^1\text{H}$  NMR (DMSO- $d_6$ )  $\delta$  (ppm): 1.226 (m, 12H,  $-\text{CH}_2-$ ), 1.898 (m, 4H,  $-\text{CH}_2-$ ), 4.898 (t, 4H,  $\text{N}^+\text{CH}_2-$ ), 8.138 (4H,  $-\text{CH}=\text{CH}-$ ), 6.447–6.484

(d,  $J = 7.4$  Hz, 4H, Ar), 6.978 (m, 8H, Ar), 7.162 (m, 10H, Ar), 7.358–7.396 (d,  $J = 7.6$  Hz, 4H, Ar), 7.689–7.733 (d,  $J = 8.8$  Hz, 2H, Ar), 7.845–7.889 (d,  $J = 8.8$  Hz, 2H, Ar), 7.986 (t, 2H, Ar), 8.209–8.246 (d,  $J = 7.4$  Hz, 2H, Ar), 8.445 (t, 4H, Ar), 8.980–9.022 (d,  $J = 8.4$  Hz, 1H, Ar), 9.242–9.275 (d,  $J = 6.6$  Hz, 1H, Ar).

Low resolution MS,  $m/z$ : calc. 937.28  $[\text{M} - 2\text{I}]^{2+}$ , measured 937.6  $[\text{M} - 2\text{I}]^{2+}$ .

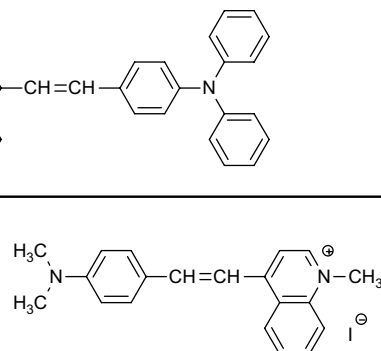
Elemental analysis: calc. 68.572% C, 5.416% H, 4.704% N, measured 65.18% C, 5.510% H, 4.710% N.

2.2.2.13. Dye **D5** – 1,5-bis[4-(2-(4-(N,N-diphenylamino)phenyl)ethenyl)quinolinyl]-pentane diiodide.



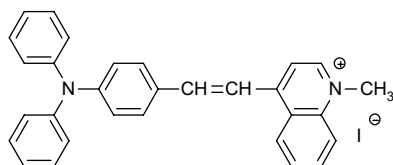
$^1\text{H}$  NMR (DMSO- $d_6$ )  $\delta$  (ppm): 1.586 (m, 2H,  $-\text{CH}_2-$ ), 1.897 (m, 4H,  $-\text{CH}_2-$ ), 4.934 (t, 4H,  $\text{N}^+\text{CH}_2-$ ), 8.150 (4H,  $-\text{CH}=\text{CH}-$ ), 6.597 (t, 4H, Ar), 6.893 (m, 10H, Ar), 7.121 (m, 10H, Ar), 7.260–7.300 (d,  $J = 8.0$  Hz, 2H, Ar), 7.359–7.399 (d,  $J = 8.0$  Hz, 4H, Ar), 7.688–7.732 (d,  $J = 8.8$  Hz,

2.2.2.15. Dye **D7** – 1-methy- 4-(4-(N,N-dimethylamino)styryl)quinolinium iodide.



$^1\text{H}$  NMR (DMSO- $d_6$ )  $\delta$  (ppm): 3.063 (s, 6H, N-CH $_3$ ), 4.435 (t, 3H, N $^+$ CH $_3$ ), 7.966–8.044 (d,  $J$  = 15.6 Hz, 2H, -CH=), 6.799–6.841 (d,  $J$  = 8.4 Hz, 2H, Ar), 7.841–7.885 (d,  $J$  = 8.8 Hz, 2H, Ar), 8.202 (m, 2H, Ar), 8.315–8.352 (d,  $J$  = 7.4 Hz, 2H, Ar), 9.000–9.042 (d,  $J$  = 8.4 Hz, 2H, Pyr), 9.085–9.119 (d,  $J$  = 6.8 Hz, 2H, Pyr).

2.2.2.16. Dye **D8** –1-methyl-4-(4-(N,N-diphenylamino)styryl)quinolinium iodide.



$^1\text{H}$  NMR (DMSO- $d_6$ )  $\delta$  (ppm): 4.500 (s, 3H, N $^+$ CH $_3$ ), 7.841–7.896 (d,  $J$  = 11.0 Hz, 2H, -CH=), 6.595–6.635 (d,  $J$  = 8.0 Hz, 2H, Ar), 6.942–6.985 (d,  $J$  = 8.6 Hz, 4H, Ar), 7.168 (t, 6H, Ar), 7.361–7.400 (d,  $J$  = 7.8 Hz, 4H, Ar), 8.014 (t, 1H, Ar), 8.241 (t, 1H, Ar), 8.385–8.413 (1H, Ar), 8.426–8.446 (1H, Ar).

Low resolution MS,  $m/z$ : calc. 413.54  $[\text{M} - 2]^+$ , measured 413.4  $[\text{M} - \text{I}]^+$ .

Elemental analysis: calc. 66.673% C, 4.663% H, 5.183% N, measured 66.14% C, 5.041% H, 5.440% N.

### 3. Results and discussion

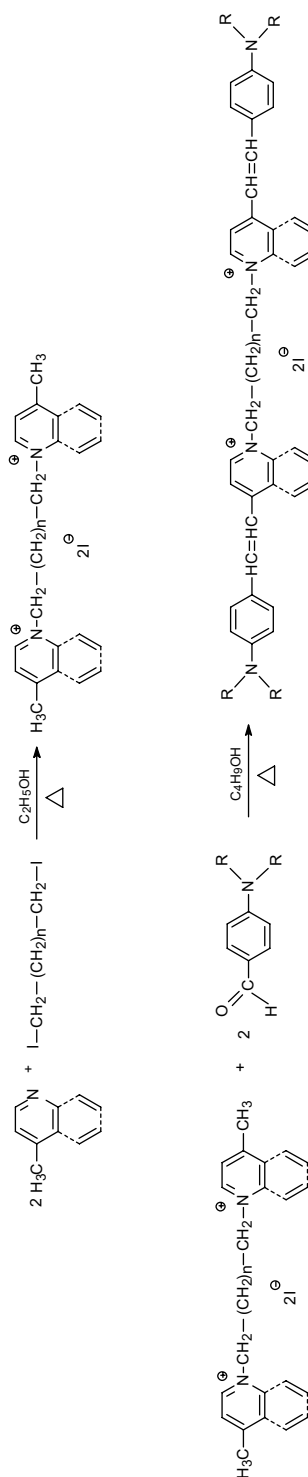
#### 3.1. Molecular design and synthetic procedures

As a part of our investigations [13,15,16] on hemicyanine dyes as photoinitiators for free radical polymerization operating in the visible light region we have synthesized homodimeric hemicyanine dyes. These dyes coupled with alkyltriphenylborate anion can be considered as good sensitizers for vinyl monomers' polymerization.

For the synthesis of homodimeric styrylpyridinium and styrylquinolinium dyes, the reaction route presented in Scheme 1 was applied.

Structure characteristics of obtained dyes are explained in Section 2. The quaternary salts of the dyes were synthesized by reflux of 4-methylpyridine or 4-methylquinoline with corresponding dihalogen alkane in anhydrous ethanol. The solid crude product was obtained by the evaporation of the solvent and washing with diethyl ether. The reactivity of methyl group positioned at 4-position in respect to heterocyclic nitrogen in the starting salts is sufficiently high to form corresponding styryl dyes. The di(homo)chromophoric hemicyanine dyes were obtained upon interaction of an appropriate either quinolinium or pyridinium salts with a corresponding aldehyde in *n*-butanol in the presence of piperidine as catalyst. Our investigation revealed that using *n*-butanol instead of methanol makes possible the separation of the dye directly after cooling the reaction mixture to a room temperature. The dyes were purified by crystallization from appropriate solvents. The yield of the reaction oscillated in the range of 57–97% and was depended on the type of an alkylammonium salt. Practically, in all cases the highest reaction yield was obtained for pyridinium derivatives.

The structure and purity of the prepared compounds were confirmed by  $^1\text{H}$  NMR, MS spectroscopy, thin layer chromatography and elemental analysis. The structural analysis of the dyes is explained in Section 2. It is noteworthy that for almost all compounds the  $^1\text{H}$  NMR spectra display two characteristic doublets localized at chemical shifts about 7 and 8 ppm. They are attributed to both vinyl hydrogen atoms. The coupling between these protons ( $J \approx 15$  Hz) indicates the *trans* form of the ground state of the synthesized dyes. The data characterizing the structure of all prepared compounds also show all relevant protons. The inspection



Scheme 1. A general route for the synthesis of homodimeric hemicyanine dyes.

**Table 1**  
Characterization data of hemicyanine dyes tested

No	M.p. (°C)	Yield (%)	Molecular formula	Molecular mass (g/mol)
<b>D1</b>	204–206	68	C <sub>41</sub> H <sub>42</sub> N <sub>4</sub> I <sub>2</sub>	844
<b>D2</b>	208–209	76	C <sub>43</sub> H <sub>46</sub> N <sub>4</sub> I <sub>2</sub>	872
<b>D3</b>	220–223	81	C <sub>48</sub> H <sub>56</sub> N <sub>4</sub> I <sub>2</sub>	942
<b>D4</b>	218–220	87	C <sub>61</sub> H <sub>50</sub> N <sub>4</sub> I <sub>2</sub>	1092
<b>D5</b>	200–202	83	C <sub>63</sub> H <sub>54</sub> N <sub>4</sub> I <sub>2</sub>	1120
<b>D6</b>	202–205	82	C <sub>68</sub> H <sub>64</sub> N <sub>4</sub> I <sub>2</sub>	1190
<b>D7</b>	267–270	97	C <sub>20</sub> H <sub>21</sub> N <sub>2</sub> I	416
<b>D8</b>	205–208	83	C <sub>30</sub> H <sub>25</sub> N <sub>2</sub> I	540
<b>P1</b>	198–203	98	C <sub>33</sub> H <sub>38</sub> N <sub>4</sub> I <sub>2</sub>	744
<b>P2</b>	287–288	98	C <sub>35</sub> H <sub>42</sub> N <sub>4</sub> I <sub>2</sub>	772
<b>P3</b>	286–287	90	C <sub>40</sub> H <sub>52</sub> N <sub>4</sub> I <sub>2</sub>	842
<b>P4</b>	244–245	96	C <sub>53</sub> H <sub>46</sub> N <sub>4</sub> I <sub>2</sub>	992
<b>P5</b>	234–235	97	C <sub>55</sub> H <sub>50</sub> N <sub>4</sub> I <sub>2</sub>	1020
<b>P6</b>	194–195	96	C <sub>60</sub> H <sub>60</sub> N <sub>4</sub> I <sub>2</sub>	1090
<b>P7</b>	248–250	88	C <sub>16</sub> H <sub>19</sub> N <sub>2</sub> I	366
<b>P8</b>	190–191	54	C <sub>26</sub> H <sub>23</sub> N <sub>2</sub> I	490

of the data presented in Table 1 shows that the melting points for all compounds are rather sharp. This can indicate the high purity of the synthesized dyes.

### 3.2. Spectroscopic studies

The UV–vis and steady-state fluorescence spectroscopic investigations show the solvent-sensitive absorption and emission, which result from the Intramolecular Charge Transfer (ICT) nature of the chromophores present in the dimeric structure of molecules.

Figs. 1–5 show the illustrative electronic absorption and the fluorescence emission spectra for the selected hemicyanine dyes in solvents of different polarity. Table 2 collects the values of both the absorption and the emission maximum positions and molar absorption coefficients for the tested dyes.

UV–vis spectroscopic measurements of tested dimers (Figs 1–3) show broad absorption bands in the range of 460–560 nm corresponding to the  $S_0 \rightarrow CT$  transition attributed to an Intramolecular Charge Transfer (ICT) involving the electron lone pair of the amino nitrogen and the cationic pyridinium (or quinolinium) nitrogen moiety [12,16,22]. The shortest wavelength bands are attributed to the  $\pi \rightarrow \pi^*$  transitions. The molar absorption coefficients of the CT bands oscillate between 9400 and 75,000  $M^{-1}cm^{-1}$  for series D and between 15,000 and 100,000  $M^{-1}cm^{-1}$  for series P. The molar absorption coefficients of shortest wavelength bands range from

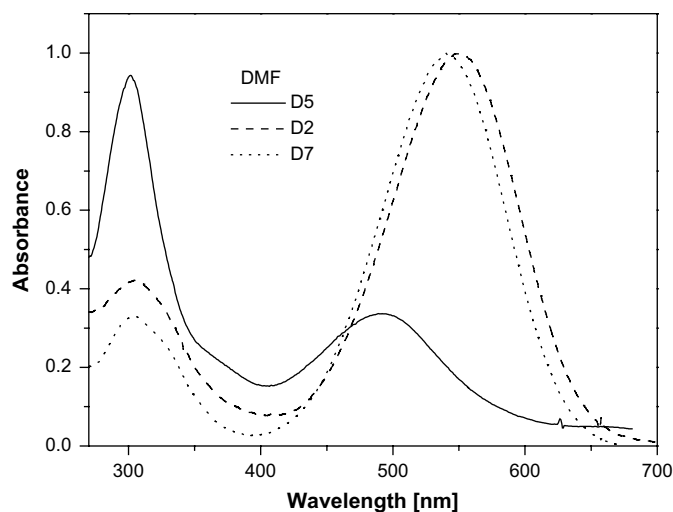


**Fig. 1.** Electronic absorption spectra of selected dyes (marked in the figure) in DMF at 293 K. The chromophores are end-capped with different donor groups and possess the same acceptor moiety.

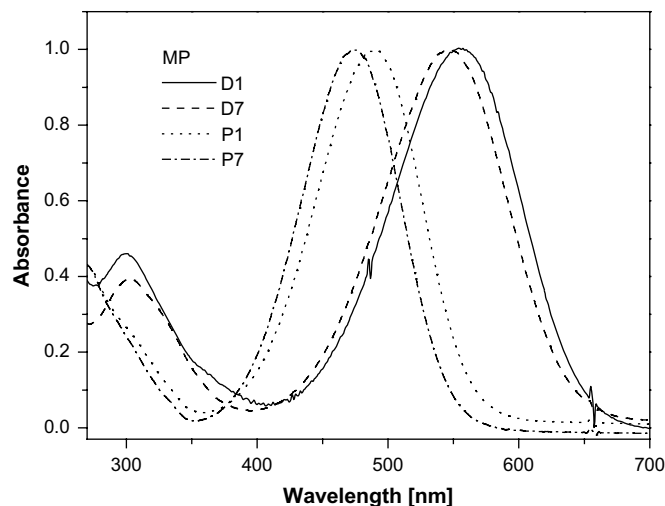


**Fig. 2.** Electronic absorption spectra of selected dyes (marked in the figure) in MP at 293 K. The applied dyes possess the same donor group and various acceptor groups.

12,000 to 67,000  $M^{-1}cm^{-1}$  for series D and from 20,000 to 48,000  $M^{-1}cm^{-1}$  for series P. Generally, the molar absorption coefficient of tested dicationic dyes is about twice as high as measured for their monomeric equivalents.

The inspection of the illustrative absorption spectra, presented in Figs. 1–3, shows that the position and the intensity of absorption bands depend on the molecular structure of the dye. Fig. 1 presents the normalized absorption spectra in DMF of the three selected dyes from group D.

The absorption spectra of tested compounds are affected by the type of dialkyl(aryl)amino group in dye molecule. In general, there is a blue shift observed in absorption maxima of tested dyes with the exchange of dimethylamino group on diphenylamino one (Table 2). For example, in DMF the maximum absorption position (Table 2) shows a value of spectral shift more than 20 nm and this indicates that the electronic transition of the hemicyanine chromophores is significantly perturbed by the electron donor moiety structure. The exchange of the dimethylamino group on diphenylamino causes also the decrease of the molar absorption coefficients of the CT band and simultaneous increases in the molar absorption coefficients of the shortest wavelength band. In general,

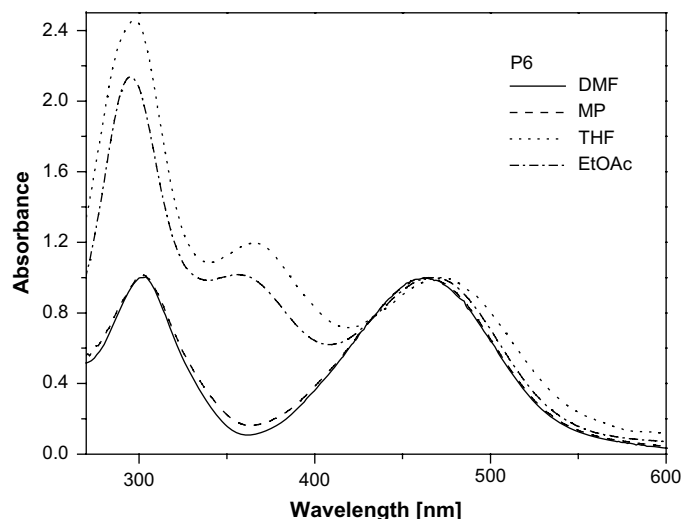


**Fig. 3.** Electronic absorption spectra of P6 dye in solvents of different polarity at 293 K.



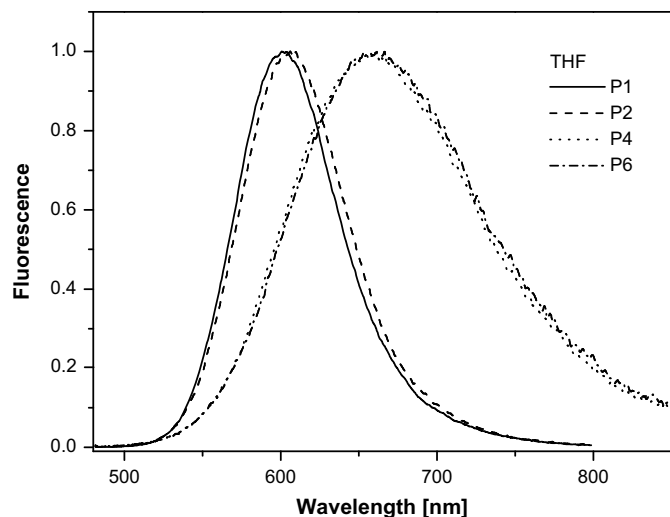


**Fig. 4.** Normalized fluorescence spectra of selected dyes (marked in the figure) in THF at 293 K. The chromophores are end-capped with different donor groups and possess the same acceptor moiety.

the better electron donor is the substituent, the more bathochromically is shifted the CT absorption band.

The analysis of the data collected in Table 2 also indicates that the position of the CT absorption band depends on the electron acceptor part of the dye molecule. The exchange of pyridinium moiety on quinolinium position causes a significant variation in the absorption maximum position. The maximum of absorption

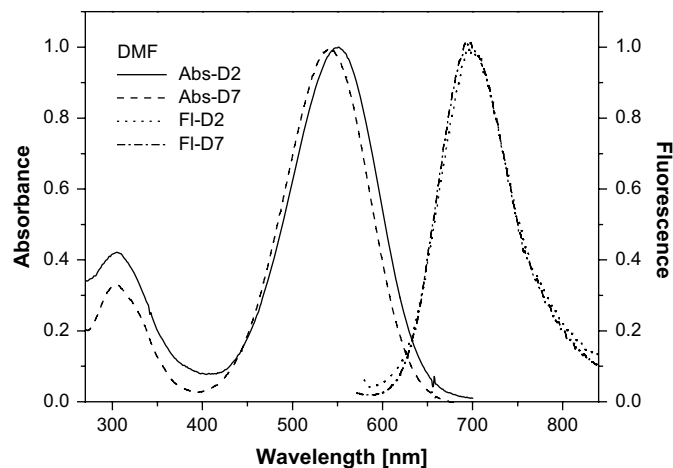


**Fig. 5.** Normalized electronic absorption and fluorescence emission spectra of the selected dyes (marked in figure). Spectra recorded in DMF and THF at 293 K.

position (Table 2) differs in some cases up to 70 nm and this indicates that the electronic transition of the hemicyanine chromophores is caused by the structure of the electron acceptor moiety. The good illustration of this influence is the dyes **D1** and **P1**. Dye **D1** absorption bands' maxima are located at 551 nm in DMF and at 555 nm in MP, whereas **P1** absorption bands' maxima are present at 485 and 490 nm, respectively. This bathochromic effect is attributed to the presence of additional benzene ring in quinolinium derivatives, causing a lesser withdrawing character of electron acceptor of this type.

**Table 2**  
Spectroscopic properties of the hemicyanine dyes tested in solvents of different polarity

Dye	$\lambda_{\text{max}}^{\text{Ab}}$ (nm), $\epsilon$ (M <sup>-1</sup> cm <sup>-1</sup> )			$\lambda_{\text{max}}^{\text{Fl}}$ (nm)	Dye	$\lambda_{\text{max}}^{\text{Ab}}$ (nm), $\epsilon$ (M <sup>-1</sup> cm <sup>-1</sup> )			$\lambda_{\text{max}}^{\text{Fl}}$ (nm)
<i>N,N</i> -Dimethylformamide (DMF; $\epsilon = 36.71$ , $n_D^{20} = 1.43047$ )									
D1	551, 54,200	305, 20,700		699	P1	485, 98,200	–		629
D2	552, 54,900	305, 20,400		700	P2	478, 91,100	–		628
D3	547, 74,300	304, 25,800		699	P3	477, 93,700	–		624
D4	522, 36,100	304, 35,000		774	P4	467, 28,500	301, 42,700		694
D5	521, 17,500	304, 38,500		764	P5	467, 38,100	301, 44,200		691
D6	522, 11,200	305, 42,100		716	P6	462, 43,300	304, 43,400		691
D7	540, 37,100	304, 12,300		697	P7	472, 51,000			624
D8	517, 9500	305, 31,500		776	P8	457, 15,200	303, 20,000		693
<i>1</i> -Methylpyrrolidin-2-one (MP; $\epsilon = 33.00$ , $n_D^{20} = 1.4700$ )									
D1	555, 52,800	301, 24,100		690	P1	490, 95,600	–		618
D2	557, 66,500	301, 28,200		695	P2	483, 94,400	–		620
D3	553, 73,700	304, 26,200		694	P3	482, 88,500	–		619
D4	528, 39,000	304, 31,700		712	P4	465, 30,400	303, 46,100		663
D5	528, 18,500	304, 42,000		728	P5	465, 43,100	303, 44,100		663
D6	523, 12,900	302, 57,600		731	P6	464, 57,300	302, 47,900		673
D7	547, 42,000	303, 16,500		690	P7	474, 43,800	–		621
D8	519, 9400	304, 31,800		766	P8	462, 16,800	303, 21,900		668
<i>Tetrahydrofuran</i> (THF; $\epsilon = 7.58$ , $n_D^{20} = 1.40716$ )									
D1	559	299		685	P1	476	360	298	601
D2	555	302		681	P2	480	–	299	603
D3	557	299		686	P3	484	366	297	605
D4	539	302		752	P4	477	366	298	657
D5	539	300		749	P5	472	366	298	666
D6	536	–		731	P6	471	365	298	658
D7	555	301		690	P7	471	367	295	614
D8	540	–		756	P8	462	367	298	655
<i>Ethyl acetate</i> (EtOAc; $\epsilon = 6.053$ , $n_D^{20} = 1.37239$ )									
D1	545	361	295	674	P1	476	–	299	597
D2	543	332	–	674	P2	478	369	295	595
D3	544	330	–	689	P3	478	368	294	591
D4	524	358	295	727	P4	468	358	295	653
D5	526	348	296	729	P5	463	355	295	656
D6	527	359	295	703	P6	467	357	295	651
D7	540	–	297	688	P7	470	365	293	594
D8	512	348	297	712	P8	458	364	295	637



It is also observed (Fig. 2, Table 2) that the monochromophoric dyes for example **D7** and **P7** in MP show  $\lambda_{\max}$  at 547 and 474 nm, respectively, while their dichromophoric equivalents (**D1** and **P1**) show absorption maxima at 555 and 490 nm. The mechanism causing the red shift observed for dichromophoric dyes in comparison to its monomeric equivalents is not clear. It may be speculated that the second electron acceptor, being in proximity to one belonging to light absorbing chromophore, causes an additional increase of electron affinity of the electron-accepting moiety of light absorbing chromophore. The red shift of the absorption maximum for the dichromophoric dyes in comparison to their monochromophoric equivalents is decreasing as the number of methylene units separating chromophores is increasing. The red shift (in DMF) for the dye with 3 methylene units (**P1**) is about 600  $\text{cm}^{-1}$ , with 5 units (**P2**) about 300  $\text{cm}^{-1}$  and with 10 units (**P3**) only 200  $\text{cm}^{-1}$ . In the case of quinolinium dichromophoric dyes the red shift (in DMF) is about 300  $\text{cm}^{-1}$  (for **D4**), 220  $\text{cm}^{-1}$  (for **D5**) and 150  $\text{cm}^{-1}$  (for **D6**). This is an additional proof of a lesser withdrawing character of quinolinium moiety in comparison to pyridinium group.

The difference between the dimers' structure is the length of the spacer between two hemicyanine chromophores. **D1, D2, D4, D5, P1, P2, P4** and **P5** have relatively short-length methylene chain between two hemicyanine moieties, and the distance between the two chromophores is in an order of several angstroms, whereas the link in **D3, D6, P3** and **P6** is relatively long (ten methylene groups), and thus the distance between the two chromophores is much larger. Generally speaking, the dyes with longer spacer show the properties more similar to their monomeric equivalents because the two chromophores are quite well separated from each other. A shorter distance between two chromophores may bring a higher possibility for "interchromophore delocalization", which is similar to the expansion of the conjugating degree of the chromophore and consequently red shifts the absorption band. Our observations are in a good agreement with the results presented in the papers published by Huang et al. who described the properties of similar types of dichromophoric hemicyanine dyes [23,24]. The specific influence of the neighboring electron-accepting group on a light absorbing molecule properties may have crucial importance on possible two-photon absorption behavior of the dyes described in this paper.

It is well-known that hemicyanine has a strong absorption band around 500 nm, which comes from the charge-transfer transition. Extensive research on hemicyanines and their derivatives in the past two decades shows that hemicyanine chromophore indicates negative solvatochromic behavior (absorption peak position blue shifts as solvent polarity increases), indicating that the ground state has larger dipole moments than excited state (Franck-Condon region) [12,22–25]. Fig. 3 shows the absorption spectra of **P6** in four different, common solvents: *N,N*-dimethylformamide (DMF), 1-methyl-2-pyrrolidinone (MP), tetrahydrofuran (THF) and ethyl acetate (EtOAc).

The shapes of spectra, as it is shown in Fig. 3, depend on the type of solvents. In THF and EtOAc, beside the CT and short-wavelength bands, an extra additional absorption peak appears at about 350–370 nm.

An important feature of hemicyanine and cyanine dyes and their derivatives is that they can easily form aggregates in appropriate solvents and confined regions (such as monolayers) [2,26]. Structurally similar dichromophoric hemicyanines have been conscientiously studied by Huang et al. [23,24]. According to the results obtained from absorption spectra of hemicyanines and the exciton theory, the usually observed a new, large blue-shifted absorption peak is originated from H-aggregates. It has been confirmed that the H-aggregates are characterized by an absorption peak around 360 nm and that the formation of H-aggregate strongly depends on the hemicyanine dye environments [27]. Thus, the strong absorption around 360 nm in EtOAc and THF probably results from the formation of the H-aggregates. The possible reason for this specific

phenomenon can be derived from a high dipole moment of the hemicyanine chromophore: weaker polar solvents do not favor the high polar solute molecule. Thus, those high polar hemicyanine molecules are not well "dissolved" in weak polar solvents but prefer to disperse into aggregates. This specific behavior in THF and EtOAc is observed for all dyes under the study, no matter whether they are in monomeric or dimeric structural form.

The dyes tested show a broad and structure less emission spectra with large Stokes shifts. The emission data for selected mono- and bischromophoric dyes under the study are given in Table 2. The steady-state fluorescence emission spectra of selected dyes in THF are presented in Fig. 4 for illustration.

Generalizing, the fluorescence spectra of hemicyanine dyes possessing *N,N*-diphenylamino substituents are more broadened in comparison to those derivatives possessing *N,N*-dimethylamino groups. From Table 2, it can be seen that the maximum of the fluorescence spectra for all chromophores is located in the region of 700–780 nm for series D and 600–680 nm for series P (an excitation wavelength 560 or 470 nm, respectively). The fluorescence maxima positions of the dyes are significantly red shifted with increasing solvent polarity. The shift depends on the dye structure and oscillates from 530 up to 840  $\text{cm}^{-1}$  (for **D1** and **D4** respectively, changing the solvent from EtOAc to DMF). The illustrative fluorescence emission spectra, presented in Fig. 4, reveal that the structure of the electron donor group in the molecule has a significant effect on the emission band position. It is apparent from the inspection of fluorescence spectra that the structure of the electron donating group changes the fluorescence maximum position (690 and 712 nm in MP for dyes **D1** and **D4** or 618 and 663 nm for dyes **P1** and **P4** in MP respectively, see Table 2). It is also observed that the fluorescence emission spectra of the hemicyanine dyes from the group D are red shifted in comparison to the dyes from group P.

The difference in energy between the absorbed and emitted radiation is known as the Stokes shift [21]. Stokes shift is attributed to a different charge distribution (or geometry) in the excited state compared to the ground state [9,21]. On the basis of quantum chemical calculations, Fromherz [28] reported for the hemicyanine dyes that the positive charge of the chromophore is displaced upon the excitation from the pyridinium moiety towards the amino moiety. Fluorescent molecules such as that described in this paper have the possibility of multiple structures' formation caused by the possible molecule fragments' rotation about bonds linking molecule various fragments. It means that the geometry of the ground state differs from their excited state geometry. Stokes shift is one of the quantitative parameters which is useful to understand the origin of the variation of spectral shift in organic solvents and is an important characteristic of change of the dipole moment upon excitation and thus indicates the extent of charge transfer in the excited state [29].

The normalized absorption and emission spectra of two selected dyes, in DMF, are presented in Fig. 5 for illustration.

It is apparent from the inspection of the spectra presented in Figs. 4 and 5 and the data collected in Tables 2 and 3 that there is a significant variation in the Stokes shift caused by the change of

**Table 3**  
Stokes shift for tested dyes

Dye	$\bar{\nu}(\text{cm}^{-1})$				Dye	$\bar{\nu}(\text{cm}^{-1})$			
	DMF	MP	THF	EtOAc		DMF	MP	THF	EtOAc
<b>D1</b>	3843	3525	3291	3512	<b>P1</b>	4720	4227	4369	4258
<b>D2</b>	3830	3565	3334	3579	<b>P2</b>	4997	4575	4250	4114
<b>D3</b>	3975	3674	3376	3869	<b>P3</b>	4939	4592	4132	4000
<b>D4</b>	6237	4894	5255	5329	<b>P4</b>	7004	6422	5744	6054
<b>D5</b>	6105	5061	5202	5294	<b>P5</b>	6941	6422	6171	6354
<b>D6</b>	5117	5441	4977	4751	<b>P6</b>	7173	6693	6034	6052
<b>D7</b>	4171	3789	3525	3984	<b>P7</b>	5161	4994	4945	4442
<b>D8</b>	6569	6139	5291	5486	<b>P8</b>	7452	6675	6378	6135

the solvent polarity. This suggests that the Stokes shift increases as the solvent polarity increases. This behavior is the well-known manifestation of the charge transfer character of the solvent relaxed emissive state. The Intramolecular Charge Transfer (ICT) state is derived following relaxation of the initially formed Franck–Condon excited state. It is clearly visible that dyes possessing strong electron donor substituents such as *N,N*-dialkylamino groups are characterized by smaller Stokes shift than those possessing weak electron donor groups.

#### 4. Summary

A series of hemicyanine homodimers, in which two identical chromophores are linked *via* three, five and ten methylene groups, have been synthesized and their electronic absorption and steady-state fluorescence spectra have been investigated. The dyes were obtained by condensation of *p*-aminobenzaldehyde and corresponding bis-quaternary salts. The UV–vis and steady-state fluorescence spectroscopic investigations show a solvent dependent absorption and emission, which result from the intramolecular charge transfer (ICT) nature of the chromophores present in the dimeric structure.

#### Acknowledgment

This work was supported by the Ministry of Science and High Education **N N204 054135**. We are very much indebted to Professor Bronisław Marciniak from Adam Mickiewicz University (UAM) for helping in MS measurements. The authors wish to thank Professor Jerzy Pączkowski for participation in discussion and preparation of the paper.

#### References

- [1] Nenkataraman K. The chemistry of synthetic dyes, vol. 2. New York, San Francisco, London: Academic Press; 1952. p. 1143.
- [2] Mishra A, Behera RK, Behera PK, Mishra BK, Behera GB. Cyanines during the 1990s: a review. *Chem Rev* 2000;100:1973–2012.
- [3] Wang Q-C, Qu D, Ren J, Xu L, Liu M, Tian H. New benzo[e]indolinium cyanine dyes with two different fluorescence wavelengths. *Dyes Pigments* 2003;59:163–72.
- [4] Wang J, Cao W-F, Su J-H, Tian H, Huang Y-H, Sun Z-R. Syntheses and nonlinear absorption of novel unsymmetrical cyanines. *Dyes Pigments* 2003;57:171–9.
- [5] Gawinecki R, Trzebiatowska K. The effect of the amino group on the spectral properties of substituted styrylpyridinium salts. *Dyes Pigments* 2000;45:103–7.
- [6] Phillips AP. Condensation of aromatic aldehydes with  $\alpha$ -picoline methiodide. *J Org Chem* 1947;12:333–41.
- [7] Phillips AP. The attempted condensation of aromatic aldehydes with  $\beta$ -picoline methiodide. *J Am Chem Soc* 1952;74:3296–7.
- [8] Ephardt H, Fromherz P. Fluorescence and photoisomerization of an amphiphilic aminostilbazolium dye as controlled by the sensitivity of radiationless deactivation to polarity and viscosity. *J Phys Chem* 1989;93:7717–25.
- [9] Zhao CF, Gvishi R, Narang U, Ruland G, Prasad PN. Structures, spectra, and lasing properties of new (aminostyryl)pyridinium laser dyes. *J Phys Chem* 1996;100:4526–32.
- [10] Gromov SP, Fedorova OA, Ushakov EN, Buevich AV, Baskin II, Pershina YV. Total synthesis of the mycotoxin (–)-zearalenone based on macrocyclisation using a cinnamyl radical intermediate. *J Chem Soc Perkin Trans 2* 1992:1323–8.
- [11] He GS, Bhawalkar JD, Zhao CF, Prasad PN. Optical limiting effect in a two-photon absorption dye doped solid matrix. *Appl Phys Lett* 1995;67:2433–5.
- [12] Jędrzejewska B, Kabatc J, Pączkowski J. 1,3-Bis[4-(*p*-aminostyryl)-pyridinyl]-propane dibromide derivatives: synthesis and spectroscopic investigation. *Dyes Pigments* 2007;73:361–7.
- [13] Kabatc J, Jędrzejewska B, Pączkowski J. Hemicyanine *n*-butyltriphenylborate salts as effective initiators of free radical polymerization photoinitiated via photoinduced electron transfer process. *J Polym Sci Part A Polym Chem* 2003;41:3017–26.
- [14] Kabatc J, Jędrzejewska B, Pączkowski J. Asymmetric cyanine dyes as fluorescence probes and visible-light photoinitiators of free radical polymerization processes. *J Appl Polym Sci* 2006;1:207–17.
- [15] Kabatc J, Jędrzejewska B, Pączkowski J. New heterobicationic hemicyanine dyes: synthesis, spectroscopic properties, and photoinitiating ability. *J Polym Sci Part A Polym Chem* 2006;44:6345–59.
- [16] Jędrzejewska B, Kabatc J, Pietrzak M, Pączkowski J. Styrylpyridinium borate salts as dye photoinitiators of free radical polymerization. *J Polym Sci Part A Polym Chem* 2002;40:1433–40.
- [17] Gawinecki R, Andrzejak S, Puchała A. Efficiency of the Vilsmeier–Haack method in the synthesis of *p*-aminobenzaldehydes. *Org Prep Proced Int* 1998;30:455.
- [18] Narang U, Zhao CF, Bhawalkar JD, Bright FV, Prasad PN. Characterization of a new solvent-sensitive two-photon-induced fluorescent (aminostyryl) pyridinium salt dye. *J Phys Chem* 1996;100:4521–5.
- [19] Hartwell JL, Pogorelskin MA. Some quaternary ammonium salts of heterocyclic bases. III. Bis-quaternary ammonium salts. *J Am Chem Soc* 1950;72:2040–4.
- [20] Mishra A, Haram NS. New push–pull type dendritic stilbazolium dyes: synthesis, photophysical and electrochemical investigation. *Dyes Pigments* 2004;63:191–202.
- [21] Kovalska VB, Kryvorotenko DV, Balanda AO, Losytskyy MYu, Tokar VP, Yarmoluk SM. Fluorescent homodimer styrylcyanines: synthesis and spectral-luminescent studies in nucleic acids and protein complexes. *Dyes Pigments* 2005;67:47–54.
- [22] Mishra JK, Behera GB, Krishna MMG, Periasamy N. Time-resolved fluorescence studies of aminostyryl pyridinium dyes in organic solvents and surfactant solutions. *J Lumin* 2001;92:175.
- [23] Huang Y, Cheng T, Li F, Huang C-H, Wang S, Huang W, et al. Photophysical studies on the mono- and dichromophoric hemicyanine dyes III. Ultrafast fluorescence up-conversion in methanol: twisting intramolecular charge transfer and “two-state three-mode” model. *J Phys Chem B* 2002;106:10041–50.
- [24] Huang Y, Cheng T, Li F, Luo C, Huang C-H, Cai Z, et al. Photophysical studies on the mono- and dichromophoric hemicyanine dyes II. Solvent effects and dynamic fluorescence spectra study in chloroform and in LB films. *J Phys Chem B* 2002;106:10031–40.
- [25] Habashy MM, El-Sawawi F, Antonious MS, Sherif AK, Abdel-Mottaleb MSA. *Indian J Chem Sect A* 1985;24:908.
- [26] Song Q, Evans CE, Bohn PW. Spectroscopic characterization of aggregation behavior in hemicyanine dye monolayer and multilayer systems. *J Phys Chem* 1993;97:13736–41.
- [27] Evans CE, Song Q, Bohn PW. Influence of molecular orientation and proximity on spectroscopic line shape in organic monolayers. *J Phys Chem* 1993;97:12302–8.
- [28] Fromherz P. Monopole–dipole model for symmetrical solvatochromism of hemicyanine dyes. *J Phys Chem* 1995;99:7188–92.
- [29] Beilenson B, Hamer FM. 5-Chloro- and 5-bromo-1-methylbenzthiazole and cyanine dyes prepared from them. *J Chem Soc* 1936:1225–31.